TELKOMNIKA Indonesian Journal of Electrical Engineering
Vol. 12, No. 9, September 2014, pp. 6526 ~ 6533
DOI: 10.11591/telkomnika.v12i9.4676

Application of Magnetic Integrated Technology in Controllable Reactor of Transformer Type

Jianning Yin*, Mingxing Tian, Guohan Yin
School of Automation & Electrical Engineering, Lanzhou Jiaotong University,
Lanzhou Gansu 730070, China
*Corresponding author, e-mail: yin200809307@163.com

Abstract

There is the magnetic coupling among control windings of controllable reactor of transformer type (CRT), the decoupling integrated magnetic technology is applied to the structure design of CRT in this paper. To realize the decoupling among the control windings we propose a magnetic integrated structure of CRT by providing low magnetic resistance magnetic circuit for control windings magnetic flux. The winding leakages of this structure are calculated, its inductance-transformer equivalent circuit is also established, and the equation of the coupling degree of control windings and no-load current with the lateral column air gap size are deduced. The simulation model for a CRT is fabricated with MATLAB/SIMULINK. Simulation and analysis results shows that when increasing the air gap, the magnetic coupling between the control windings decreases apparently, the utilization ratio of windings current is also raised. The simulation results verify the effectiveness of this method by controlling the lateral column air gap size to achieve the purpose of decoupling.

Keywords: *controllable reactor of transformer type, magnetic integration, simulation analysis, utilization*

1. Introduction

In the EHV transmission system, in order to solve the problem of reactive power balance, reactive power compensation device must be installed [1-3]. Controllable reactor of transformer type (CRT) is a new multi-winding reactive power compensation device; the working principle diagram of CRT is shown as Figure 1 [4-6].

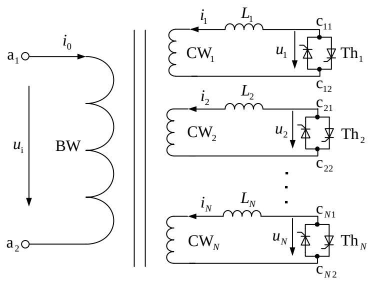

Figure 1. The Working Principle Diagram of CRT

In Figure 1, the purpose of the reactive power capacity with continuous smooth adjustment of CRT can be achieved by adjusting the size of conduction angle of the anti-parallel thyristors series in control winding loop, and the current harmonic content is small of CRT [7, 8]. However, because it has multiple control windings, there is a magnetic coupling among the control windings, which leads to the subsequent control winding input will makes the control winding current utilization rate is decline of have been put into operated, in order to improve the control winding current utilization and make the CRT reliable work, reference [9] pointes out that the structural design of the CRT must follow the design principles of “high impedance and weak coupling”.

Received October 8, 2013; Revised Apr 28, 2014; Accepted June 6, 2014

In this paper, aiming at the problem of magnetic coupling among the control windings, the integrated magnetic structure of CRT which is based on the magnetic integration technology is proposed, this structure achieves the decoupling of the control windings by providing a low reluctance magnetic circuit [10-12]; The simulation example of the relationship between jamb air gap size and degree of coupling for this structure shows that the structure can weak the magnetic coupling among the control windings, improve utilization of the winding current. Generally this structure also can be easily extended to the structure of the multiple control windings, provides a reference for the further application of magnetic integration technology.

2. Magnetic Integration Structure of CRT

In magnetic integration technology, the decoupling integrated method which provides a low reluctance magnetic can achieve the decoupling of multi-windings [13]. this method is applied to the structural design of CRT, and a kind of integrated magnetic structure of CRT is proposed and shown as Figure 2.

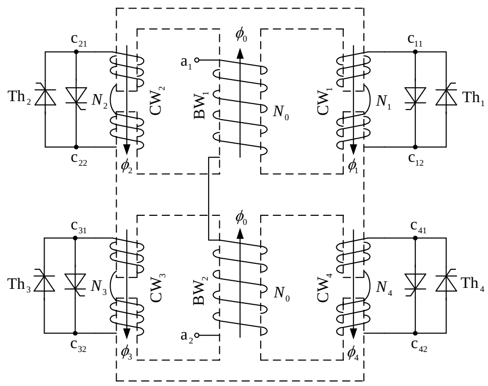

Figure 2. Integrated Magnetic Structure of CRT

In Figure 2, a_1, a_2 are two ports of the working winding, and paralleled to the power grid, the power grid voltage between the two ports; c_{ij} (i=1,2,3,4; j=1,2)is the j-th port of control winding CW_i, the anti-parallel thyristors are used in series with both ports of each control winding, reactive power of CRT can be adjusted by thyristors. Core column around the working winding and iron yoke up and down are low magnetic resistance, side legs around control windings are gapped to increase the reluctance, so that a large part of magnetic flux which is generated by the control windings constitutes a closed loop through the low magnetic resistance magnetic circuit with its column, while only a small amount of magnetic flux flowing through magnetic circuit in other control windings, which will weak the direct coupling among the control windings, because the working windings around the upper and lower center column are connected in series, the inputs of subsequent control windings will lead to the increasing of working wingding current, so that the magnetic flux generated by the working winding will also raise, in turn, this will effect the control winding current which has been put into operated. We define it as an indirect coupling; this degree of coupling is small. If we don’t consider the indirect coupling, the coupling among the control windings of this structure is small, and the principle “weak coupling” among different control windings is achieved.

3. The Calculation of Coupling Degree

According to Ohm's law of magnetic circuit, the equivalent magnetic circuit of magnetic integration structure of the CRT showed in Figure 2 is shown as Figure 3.

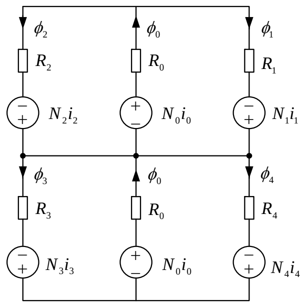

Figure 3. Equivalent magnetic circuit of magnetic integrated structure

In Figure 3, R_0 is the magnetic resistance of center column; $R_i(i=1,2,3,4)$ is magnetic resistance(including reluctance of air gap) of the side column around control winding CW_i ; N_0 is the half turns of working winding; N_i is the turns of control winding CW_i . Make $R_1=R_2=R_3=R_4=R$, in case of without considering the indirect coupling among control windings, the degree of coupling between control winding CW_1 and control winding CW_2 is:

$$k_{12}=\frac{R_0}{R_0+R}=\frac{\mu_0 l}{2\mu_0(h+2r_{co})+(\mu-\mu_0)\delta} \quad (1)$$

Where, μ_0 and μ is permeability of the air gap and core respectively; l is the calculative length(including the center column height and length of the iron yoke) of the center column magnetic resistance; δ is the size of air gap for side column; h is the height of side column; r_{co} is the radius of the core columns.

In a similar way, the degree of coupling between control winding CW_3 and control winding CW_4 is:

$$k_{34}=\frac{\mu_0 l}{2\mu_0(h+2r_{co})+(\mu-\mu_0)\delta} \quad (2)$$

And,

$$k_{13}=k_{14}=k_{23}=k_{24}=0 \quad (3)$$

It can be seen from the formula (1) and (2) that the degree of coupling among control windings decreases with the increasing of air gap for the side column when without considering the indirect coupling among control windings.

4. Equivalent Circuit of CRT

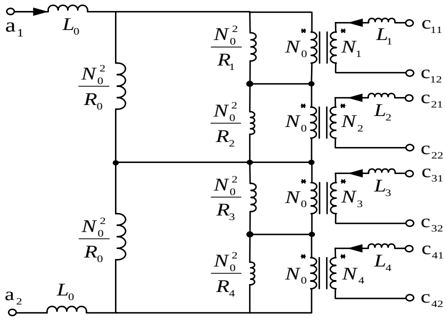

Figure 4. Inductance-transformer Equivalent Circuit

According to the established method of equivalent circuit for integrated magnetic component, with the number of turn N_0 for reference, the inductance-transformer equivalent circuit of magnetic integrated structure of CRT showed in Figure 2 now is shown as Figure 4 [14].

In Figure 4, L_0 is the leakage inductance half of the working winding; L_i is the leakage inductance of control winding CW_i, all transformers are ideal transformer, only acts as impedance transformation. Based on the equivalent circuit shown in Figure 4, the relationship of no-load current RMS with the size of the air gap can be calculated when the control winding turns of CRT are imputed N_0 is:

$$i_{00} = \frac{U_0}{\dfrac{4\omega\omega\mu_0 A N_0^2}{2\mu_0 l + (h + 2r_{co})\mu_0 + (\mu - \mu_0)\delta} + 2\omega\omega_0} \tag{4}$$

Where, U_0 is RMS of power grid voltage; A is the cross sectional area of core columns; ω is angular frequency.

It can be seen from formula (4) that no-load current i_{00} increases with the raise of the size of air gap δ for side column.

5. Calculation of Leakage Inductance

The magnetic integrated structure of CRT shown as Figure 2 are symmetric, therefore, it is based on the working winding BW_1 and control winding CW_1 as an example that to calculate the leakage inductance, which is shown as Figure 5.

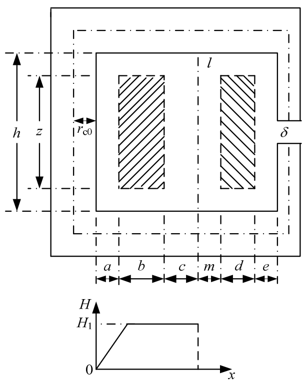

Figure 5. Magnetic Field Intensity Distribution

The Figure 5 is the core cross-sectional view and a magnetic field intensity distribution figure of working winding BW_1 and control winding CW_1. In Figure 5, h is the height of iron core window; z is the equivalent height of winding; a is the insulation distance of working winding to the center column; b is the thickness of working winding consider canceling turn insulation; d is the thickness of control winding consider canceling turn insulation; e is the insulation distance of control winding to the side column; δ is the size of air gap. Setting the line l as leakage magnetic flux distribution boundary of working winding and control winding, c is the distance of working winding to the boundary, m is the distance of control winding to the boundary.

The i_0 is the current of working winding, i_1 is the current of control winding, select the inside edge of the center column as the zero reference. According to the Ampere's law, there are:

In the area $a \sim b$, magnetic field strength increases linearly along the x direction, the expression of magnetic field strength is:

$$H_{bx} = H_0 \frac{x}{b} = \frac{N_0 i_0}{zb} x \tag{5}$$

In the area $a+b \sim a+b+c$, because without the increase of current, magnetic field intensity remains unchanged, the expression of magnetic field strength is:

$$H_{cx} = H_m = \frac{N_0 i_0}{z} \tag{6}$$

Magnetic energy also can be expressed by the following formula, in the area $a \sim b$,

$$\begin{aligned} W_1 &= \frac{\mu_0}{2} \int_a^b H_{ax}^2 dV = \frac{\mu_0}{2} \int_a^b \frac{N_0^2 i_0^2}{z^2 b^2} x^2 \cdot 2\pi\pi \cdot zdx \\ &= \frac{\mu_0 \pi}{zb^2} \left[\frac{1}{4}(a+b)^4 - \frac{1}{4} a^4 \right] (N_0 i_0)^2 \end{aligned} \tag{7}$$

In the area $a+b \sim a+b+c$,

$$\begin{aligned} W_2 &= \frac{\mu_0}{2} \int_{a+b}^{a+b+c} \frac{N_0^2 i_0^2}{z^2} \cdot 2\pi\pi \cdot zdx \\ &= \frac{\mu_0 \pi}{z} \left[\frac{1}{2}(a+b+c)^2 - \frac{1}{2}(a+b)^2 \right] (N_0 i_0)^2 \end{aligned} \tag{8}$$

The magnetic energy of the leakage reactance in the whole distributed region is:

$$W = W_1 + W_2 = \frac{1}{2} L_0 i_0^2 \tag{9}$$

According to simultaneous Equation (7), (8), (9), we can obtain the leakage inductance of the working winding BW_1 is:

$$\begin{aligned} L_0 &= \frac{2\pi\pi_0 N_0^2}{zb^2} \left[\frac{1}{4}(a+b)^2 - \frac{1}{4} a^2 \right] \\ &+ \frac{\mu_0 \pi N_0^2}{z} \left[\frac{1}{2}(a+b+c)^2 - \frac{1}{2}(a+b)^2 \right] \end{aligned} \tag{10}$$

In a similar way, the leakage inductance of the control winding CW_1 is:

$$\begin{aligned} L_1 &= \frac{2\pi\pi_0 N_1^2}{zd^2} \left[\frac{1}{4}(e+d)^4 - \frac{1}{4} e^4 \right] \\ &+ \frac{2\pi\pi_0 N_1^2}{z} \left[\frac{1}{2}(e+d+m)^2 - \frac{1}{2}(e+d)^2 \right] \end{aligned} \tag{11}$$

Other control winding leakage inductance can be calculated according to the formula (11). After the leakage inductances of the windings are calculated, the windings current can be simulated according to inductor-transformer equivalent circuit shown in Figure 4 of CRT.

6. Example Calculation and Simulation

The structure parameter of CRT are shown in Table 1, the turns of working winding BW_1 is $N_0 = 1600$, each control windings turn are imputed to 1600 turns, the working winding rated voltage RMS is $U_0 = 500/\sqrt{3}$ kV.

Table 1. The Structural Parameter

parameter	value(cm)	parameter	value (cm)
a	1	*h*	125
b	19	*z*	110
c	7	*d*	10
r_{co}	3.95	μ_r	2000
e	1	*m*	6

In Table 1, μ_r is relative permeability of core, other parameters which represent physical meanings are same as Figure 5.

Set the size of air gap of side columns around four control windings are equal, the cross-sectional area of side column is equal to the cross-sectional area of center column, the parameter values in Table 1 plug in type (10) can be calculated to the leakage inductance of the working winding BW_i ($i = 1,2$) is $L_0 = 2.036H$; the leakage inductance of the control winding CW_1 is $L_1 = 0.6725H$; the leakage inductance of the control winding CW_2 is $L_2 = 0.5299H$; the leakage inductance of the control winding CW_3 is $L_3 = 0.3708H$; the leakage inductance of the control winding CW_4 is $L_4 = 0.2116H$. Based on MATLAB R2009b platform, we can build simulation circuit according to Figure 4, short-circuit the control winding in turn, the current RMS of working winding and control winding can be measured [15, 16]. The Table 2, Table 3 and Table 4 of following are simulation values of windings when air gap $\delta = 0$, $\delta = 3mm$, $\delta = 7mm$ respectively.

Table 2 The Simulation Value when Air Gap $\delta = 0$

	No-load current	CW_1 short-circuit	CW_1~CW_2 short-circuit	CW_1~CW_3 short-circuit	CW_1~CW_4 short-circuit
Current of BW/A	33.43	36.36	54.47	62.90	160.70
Current of CW_1/A	0	13.76	49.25	56.87	145.30
Current of CW_2/A	0	0	49.54	57.21	146.20
Current of CW_3/A	0	0	0	24.28	152.60
Current of CW_4/A	0	0	0	0	153.60

Table 3. The Simulation Value when Air Gap $\delta = 3mm$

	No-load current	CW_1 short-circuit	CW_1~CW_2 short-circuit	CW_1~CW_3 short-circuit	CW_1~CW_4 short-circuit
Current of BW/A	60.64	68.93	86.69	106.40	164.60
Current of CW_1/A	0	45.36	70.21	86.19	133.30
Current of CW_2/A	0	0	72.28	88.73	137.20
Current of CW_3/A	0	0	0	75.43	146.40
Current of CW_4/A	0	0	0	0	151.60

Table 4. The Simulation Value when Air Gap $\delta = 7mm$

	No-load current	CW_1 short-circuit	CW_1~CW_2 short-circuit	CW_1~CW_3 short-circuit	CW_1~CW_4 short-circuit
Current of BW/A	86.84	96.43	112.00	131.30	169.00
Current of CW_1/A	0	62.38	79.67	93.28	120.20
Current of CW_2/A	0	0	84.06	98.42	126.80
Current of CW_3/A	0	0	0	96.42	138.70
Current of CW_4/A	0	0	0	0	148.40

In Table 2, Table 3 and Table 4, BW is working winding, $CW_i(i=1,2,3,4)$ is control winding. It can be seen from the simulated data above three tables that control winding CW_3 and CW_4 put into operation will impact on the currents of CW_1 and CW_2, this is because there is indirect coupling between them. It can be concluded from the compare with simulated data that in the case of other parameters are same exactly, with the air-gap increases, the load current also increases, which is fully consistent with the result of formula (4). The current utilization curves of control winding CW_1 can be obtained according to the simulated data, the curves of different size of air-gap are shown as Figure 6.

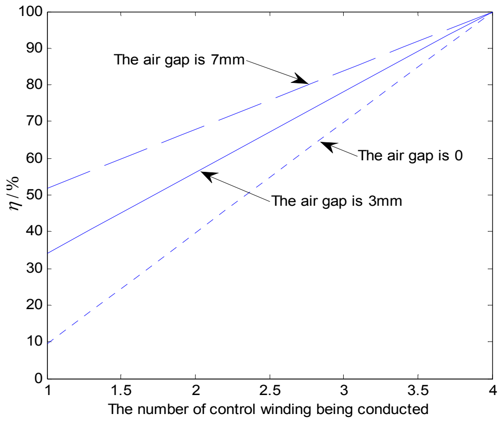

Figure 6. Curves of Current Utilization Ratio

In the Figure 6, the abscissa is an integer which means the number of control winding for being fully conducted. We can see from curves that the current utilization ratio of control winding increases with the raising of the air gap, if the air-gap of side column is bigger, the degree of coupling among control windings would be smaller, which is fully consistent with the result of formula (1) and formula (2), therefore, the size of the air gap of side column can be increased in order to achieve the control winding "weak coupling" purpose. The current utilization on the rise with input number of control winding increasing.

7. Conclusion

In this article, the decoupling integrated magnetic technology is applied to the structure design of CRT, a CRT magnetic integrated structure has been proposed. On the basis of the calculation of the leakage inductance of the windings and equivalent circuit is established, the simulation analysis of this structure on the MATLAB have been done, we get the following conclusions:

(1) The “weak coupling” design requirement among control windings of CRT can be realized by providing a low reluctance magnetic circuit.

(2) When the air gap of side column becomes bigger, the degree of coupling among control windings becomes smaller, and the utilization rate of winding current are also higher. At the same time, no-load current will increase. So rational selection of air gap size can not only make the no-load current small, but also achieve the purpose of decoupling among control windings.

(3) The method of decoupling among control windings by adjusting the air gap of side column of magnetic integrated structure of CRT is effective.

References

[1] Tian Jun, Chen Qiao-fu, Zhang Yu. Adjustable reactor with controllable load of multi-winding transformer. *Electric Power Automation Equipment*. 2010; 30(1): 32- 35.
[2] Chen Wei-xian,Chen He. Application of inter-phase shunt reactors in EHV and UHV transmission lines and suppression of resonance. *High Voltage Engineering*. 2010; 36(9): 2187-2192.
[3] ZHANG Jian-xing, WANG Xuan, LEI Xi, etal. Overview of Controllable Reactor. *Power System Technology*. 2006; 30: 269-272.
[4] ZHANG You-peng, DU Bin-xiang, TIAN Ming-xing. Research on Compensation Degree of Controllable Shunt Reactor Installed in UHV Transmission Line with Loss Considered. *High Voltage Engineering*. 2011; 37(9): 2096-2101.
[5] CHEN He, CHEN Weixian. Sustained Conduction Method of Controllable Reactor of Multiple Parallel Branch Type. *High Voltage Engineering*. 2005; 31(4): 66-68.
[6] TIAN Ming-xing, LI Qing-fu. Magnetic saturation type and transformer type controllable shunt reactor. *High Voltage Engineering*. 2003; 29(7): 26-27.
[7] Tian Mingxing, Li Qingfu. A controllable reactor of transformer type. I*EEE Transaction on Power DeliVery*. 2004; 19(4): 1718-1726.
[8] Mingxing Tian. Analysis of transformers on the concept of elementary winding. *Electrical Engineering*. 2007; 89(7): 553-561.
[9] Tian Mingxing. Basic theoretical research on controllable reactors of transformer type. PhD thesis. Xi’an: Xi’an Jiaotong University, 2005.
[10] Chen Qianhong. Research on the Application of the Magnetics-Integration Techniques in Switching Power Supply. PhD thesis. Nanjing: College of Automation Engineering Nanjing University of Aeronautics and Astronautics, 2001.
[11] ZHENG Feng, LIU Yuan-qiang, PEI Yun-qing, et al. *Criterion of Discrete Magnetics and Design Techniques of Integrated Magnetics*. Proceedings of the CSEE. 2008; 28(30):41-48.
[12] LP Wong, YS Lee, DKW Cheng. *A new approach to the analysis and design of integrated magnetics.* 16th Annual IEEE Applied Power Electronics Conference and Exposition, Anaheim, CA, USA. 2001; 1196-1202.
[13] YS Lee, LP Wong, DK Cheng. Simulation and design of integrated magnetics for power converters. *IEEE Transactions on Magnetics.* 2003; 39(2): 1008-1018.
[14] CHEN Qian-hong, RUAN Xin-bo, YAN Yang-guang. Deriving Method of Converters with Integrated magnetics and General Equivalent Circuit Model of the Magnetics. *Power Electronics*. 2004; 38(5): 48-50.
[15] PENG Bo, REN Xiao-yong, CHEN Qian-hong. Research of leakage inductance in gyrator- capacitor model. *Advanced Technology of Electrical Engineering and Energy*. 2012; 31(1): 69-73.
[16] Ding Hongfa, Zhu Qingchun. Controllable shunt reactors of hybrid transformer type and its simulations. *RELAY*. 2005; 33(10): 25-30.